

DOI: <https://doi.org/10.15407/rpra29.03.222>  
UDC 537.86

A.S. Vakula<sup>1</sup>, S.Yu. Polevoy<sup>1</sup>, K.Yu. Sova<sup>1,2</sup>,  
A.A. Girich<sup>1</sup>, S.I. Tarapov<sup>1,2,3</sup>, S.V. Nedukh<sup>1</sup>

<sup>1</sup> O.Ya. Usikov Institute for Radiophysics and Electronics NAS of Ukraine  
12, Acad. Proskury St., Kharkiv, 61085, Ukraine

<sup>2</sup> Gebze Technical University  
2, Cumhuriyet Mah. 2254 St., 41400, Gebze/Kocaeli, Turkey

<sup>3</sup> V.N. Karazin Kharkiv National University  
4, Svobody Sq., Kharkiv, 61022, Ukraine  
E-mail: vakula@ire.kharkov.ua

## MAGNETIC CORE APPLICATION IN A PLANAR RESONATOR WITH A YTTRIUM IRON GARNET FILM FOR ENHANCING STRONG PHOTON-MAGNON COUPLING

**Subject and Purpose.** This paper presents numerical simulation results on the transmission spectra of a split-ring resonator (SRR) loaded with a thin film of yttrium iron garnet (YIG). The application of a magnetic core in the SRR is proposed for increasing the photon-magnon (P-M) coupling strength. The anticrossing effect in the frequency dispersion behavior of the SRR modes and YIG film ferromagnetic resonance modes, namely SRR-YIG coupled modes, is identified. The dimensional parameters of the SRR with a magnetic core are calculated, taking care to preserve the design compactness and striving to obtain a maximum possible spin-number-normalized coupling strength for such a system. The work has been aimed at evaluating the efficiency of applying the magnetic core as a part of the planar microwave resonator to enhance the P-M coupling strength.

**Methods and Methodology.** The transmission coefficient  $|S_{21}|$  spectra of electromagnetic waves propagating through the planar resonator with the YIG film under the ferromagnetic resonance condition are numerically studied using the CST Studio Suite package in the frequency domain. The spatial distribution function of the magnetic field strength is calculated for the two scenarios of YIG film location: near the magnetic core (between the SRR and the feeding stripline) and inside the magnetic core (in the SRR center). Also, for each of these two scenarios, the transmission coefficient  $|S_{21}|$  spectra of the wave propagation through the feeding stripline in the region of SRR-YIG coupled modes are simulated with and without the magnetic core. The dispersion curves of the SRR-YIG coupled modes are obtained in analytical terms.


**Results.** It has been shown that the magnetic core application increases the P-M coupling strength 2.0 times in the scenario of YIG film location near the magnetic core (between the SRR and the feeding stripline). When the YIG film is inside the magnetic core (in the SRR center), the P-M coupling strength rises 2.3 times compared to similar cases without the magnetic core.

**Conclusions.** The suggested magnetic core application can be used to increase the P-M coupling strength in the SRR — magnetic film resonant system, striving to develop effective microwave-to-optical converters and create efficient information exchange between quantum computers.

**Keywords:** photon-magnon coupling, planar resonator, ferromagnetic resonance, transmission spectra, magnetic core.

Citation: Vakula, A.S., Polevoy, S.Yu., Sova, K.Yu., Girich, A.A., Tarapov, S.I., Nedukh, S.V., 2024. Magnetic core application in a planar resonator with a yttrium iron garnet film for enhancing strong photon-magnon coupling. *Radio Phys. Radio Astron.*, 29(3), pp. 222–228. <https://doi.org/10.15407/rpra29.03.222>

© Publisher PH "Akademperiodyka" of the NAS of Ukraine, 2024

 This is an Open Access article under the CC BY-NC-ND 4.0 license (<https://creativecommons.org/licenses/by-nc-nd/4.0/legalcode/en>)

## Introduction

Theoretical and experimental principles of photon-magnon (P-M) coupling, or interaction between the quanta of electromagnetic waves (photons) and the quanta of spin waves (magnons) are well described in [1]. The P-M coupling manifests itself in the transmission spectrum as coupled modes of both resonator and magnet under the ferromagnetic resonance (FMR) condition. Planar resonators gain more efficient P-M coupling strength and maintain a compact design [1, 2]. The problem is highly relevant today, and, as a result, many modifications of planar resonators have been developed up to date, providing significant improvements of the coupling strength efficiency [3–6].

Previously developed planar resonators have almost reached a limit in their ability to increase the spin-number-normalized P-M coupling strength,  $g_N$ , that currently stands at about 0.2 Hz [6]. Among those is the planar split-ring resonator (SRR) [2, 7–10] that has been actively studied for the last decade to find out that further transformations of the SRR shape are of little use for increasing the  $g_N$  parameter. A possible remedy is to enhance the electromagnetic coupling between the SRR and the feeding stripline.

A reasonable approach to this physical and technological problem is to increase the magnetic induction between the feeding stripline and the resonator, such as the SRR, by means of employing a high-permeability magnetic (ferrite) core [5], thus implementing the principle behind transformers in radio electronics. This being so, the present work aims at evaluating the efficiency of the magnetic core application in a planar microwave resonator to enhance the P-M coupling.

In this work, two scenarios of the yttrium iron garnet (YIG) film placement relative to the SRR are considered: between the SRR and the feeding stripline (near the magnetic core) and in the SRR center (inside the magnetic core). In both scenarios, two cases including and excluding the magnetic core are analyzed and compared. The YIG film is placed where the high-frequency magnetic field concentration is at its highest. The YIG material choice is reasoned by the widespread use of this high-spin density, low-loss ferrimagnetic material in quantum conversion technologies.

## 1. Theoretical information

We study a hybrid system consisting of the Kittel mode and the microwave cavity mode using a planar SRR with a YIG film and a feeding stripline located close to the SRR [1], see Fig. 1. The feeding stripline can excite both the resonator and the YIG film. The application of a magnetic core allows a more efficient conversion of the electromagnetic energy from the feeding stripline to the SRR via the magnetic flux in the magnetic core. The alternating magnetic flux through the circuit with cross-sectional area  $S$  is known to be [5]

$$\Phi = B S, \quad (1)$$

where  $B$  is the magnetic induction. We consider the situation when microwaves circulate in the magnetic core (Fig. 1). In this case,  $B$  is given by

$$B = \mu h, \quad (2)$$

where  $h$  is the alternating magnetic field strength in the circuit and  $\mu$  is the microwave magnetic permeability of the material filling the circuit.

The SRR with a magnetic core possesses microwave permeability  $\mu_c$ , with  $\mu_c > \mu$ . By virtue of Eq. (1), the magnetic flux density in the core increases, and so does, according to Eq. (2), the microwave magnetic induction of the core,  $B_c > B$ . The alternating magnetic field in the magnetic core induces an additional alternating current (increases the alternating current magnitude) in this SRR as against an identical SRR with the YIG film and without the magnetic core [10].

All dimensional parameters of the SRR, YIG film, and the feeding stripline hold the same, whether with the magnetic core or without. There is a dielectric insert in the SRR slit for correcting the SRR resonance frequency.

Notice that depending on the scenario, the employed 0.035 mm thick YIG film is either rectangularly shaped,  $2.6 \times 0.335$  mm when it is located between the SRR and the feeding stripline (near the magnetic core). Or, when it is in the center of the SRR (inside the magnetic core), the YIG film is cylindrical shaped, its diameter is  $d = 2.6$  mm.

Also, in both scenarios of YIG film placement, the SRR topology and dimensional parameters hold the same. The SRR is  $3.8 \times 3.8$  mm in size. The metalized part of the SRR is made of copper conductor,  $0.4 \times 0.035$  mm. The SRR slit is 0.2 mm wide and is

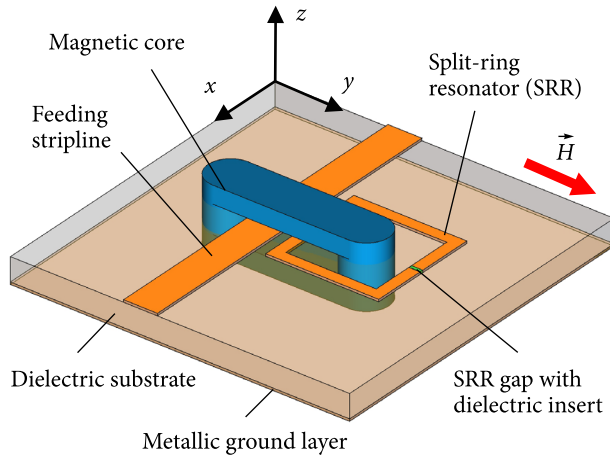


**Fig. 1.** The SRR with magnetic core

situated on the side opposite the feeding stripline (see Fig. 1). The SRR and the feeding stripline are positioned 3.33 mm apart on a 1.5 mm thick dielectric substrate of Rogers 4350B material covered at the bottom with a 0.035 mm thick copper ground layer.

The magnetic core in Fig. 1 is shaped as a closed rectangular loop. The magnetic core crosscuts the dielectric substrate with the copper ground layer in the two places: in the SRR center and outside the SRR, right behind the stripline. The magnetic core involved in our numerical simulation is assumed to be an idealized lossless magnet in the studied frequency range. Its permeability is  $\mu_c = 10$  and the permittivity is  $\epsilon_c = 1$ . To reach the specified value of the magnetic permeability, an external magnetic field beyond the FMR region of the magnetic core is applied. For the practical implementation, low-loss (in the specified frequency range) magnets, such as barium hexaferrites, can be used. In materials of this kind, the FMR absorption is observed in an external magnetic field  $H < 1000$  Oe and owes its appearance to the strong magnetic anisotropy [11]. The numerical simulation was carried out by using the CST Studio Suite package operating in the frequency domain.

For the strong-coupling regime observed in the studied SRR-YIG film system, the minima of the SRR resonance frequencies are determined by the formula [1]

$$\omega_{\pm} = \frac{1}{2} \left[ (\omega_r + \omega_p) \pm \sqrt{(\omega_r - \omega_p)^2 + 4g^2} \right], \quad (3)$$

where  $\omega_r$  is the SRR resonance frequency,  $\omega_p$  is the resonance frequency of the FMR peak in YIG ferromagnetic, and  $g$  is the P-M coupling strength value.

## 2. Results and discussion

To trace the microwave flux penetration into the YIG film through the magnetic core, let us analyze Fig. 2 and compare the spatial distributions of the induction component  $B_z(z)$  at the YIG-magnet interface for the two YIG film locations relative to the SRR. Fig. 2, *a* refers to the YIG film location between the SRR and the feeding stripline in the magnetic core absence. Fig. 2, *b* corresponds to the YIG film located in the SRR center in the magnetic core presence.

The analysis of the spatial distribution of the  $B_z(z)$  component along the  $z$ -axis (Fig. 2, *b*) shows that in the scenario of the YIG film location between the SRR and the feeding stripline, the  $|B_z|$  component increases significantly, more than 4 times, as compared to the scenario with the YIG film in the SRR center.

Fig. 3 illustrates the simulation results on the spatial distribution of the induction vector  $\vec{B}$  of the electromagnetic field in the YIG film neighborhood. Here, the YIG film is located between the SRR and the feeding stripline. Fig. 3, *b* shows that the YIG film is in an area with a high concentration of the alternating magnetic field component, where the magnitude  $|B_z|$  is at its maximum. This is an important condition for getting the P-M coupling strength at its highest. The numerical simulation of the transmission spectra of electromagnetic waves propagating through the feeding stripline and the SRR was conducted in the case of the external  $y$ -directed magnetic field  $\vec{H}$  application (see Fig. 1). The coupled photon and magnon modes in the region of the SRR resonance frequency and the YIG film FMR frequency are shown in Fig. 4.

The magnetic core presence shifts the resonance frequency to lower values (see Fig. 4), which is caused by the increased magnetic permeability of the resonator filling material ( $\mu_c > \mu$ ). In our case, the magnetic core occupies a considerable area of the SRR. As seen, the resonator modes are repulsed, and the anti-crossing effect is observed.

The calculated by formula (3) dispersion curves of the resonance frequencies  $\omega_{\pm}$  versus the external magnetic field  $\vec{H}$  are plotted in black dashed lines in Fig. 4. The P-M coupling strength  $g$  comes from expression (3). Also,  $g$  can be roughly obtained as  $g = (\omega_+ - \omega_-)/2$ , half the numerical difference between the resonance frequencies  $\omega_{\pm}$ , if an external magnetic field is applied and  $\omega_r = \omega_p$ .

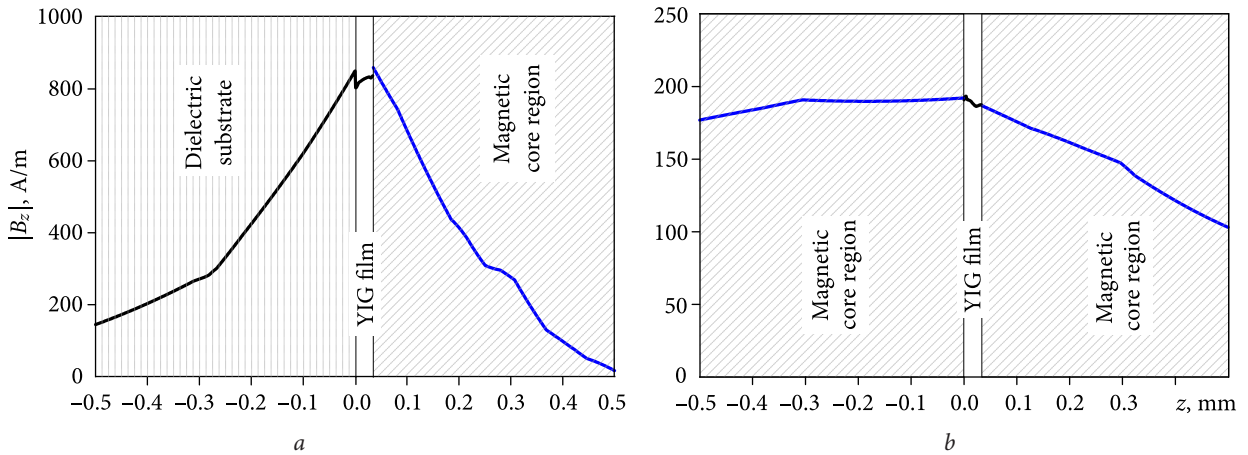


Fig. 2. Spatial distributions of the magnetic induction component  $|B_z|$ : *a* – YIG film is between the SRR and the feeding stripline (near the magnetic core) and *b* – the YIG film is in the SRR center (inside the magnetic core)

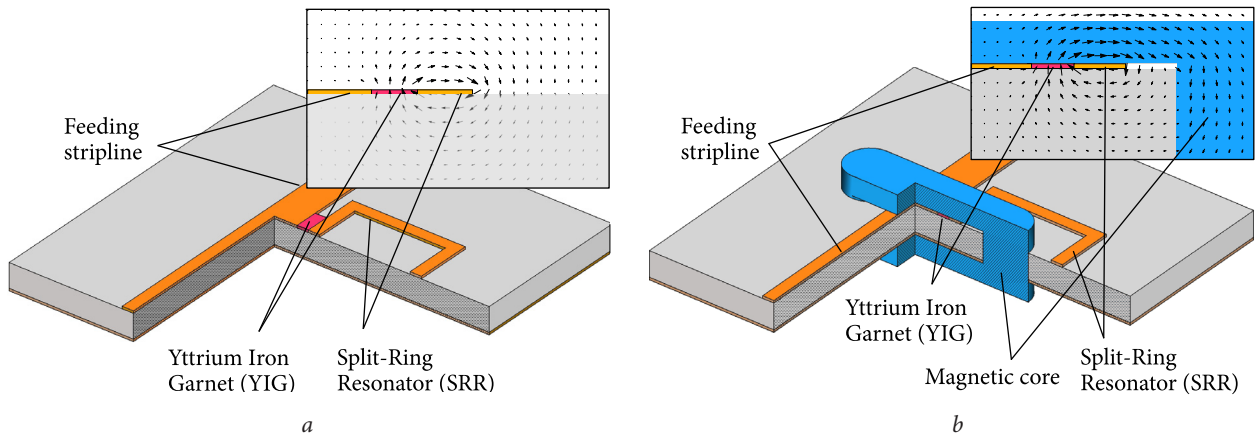


Fig. 3. The SRR with feeding stripline and YIG film between them: *a* – without and *b* – with the magnetic core. The insets show the induction vector  $\vec{B}$  spatial distributions (black arrows) at the cross-section made by the  $yz$ -cutting plane in the YIG film region and visualized with the parallelepiped-shaped cutout

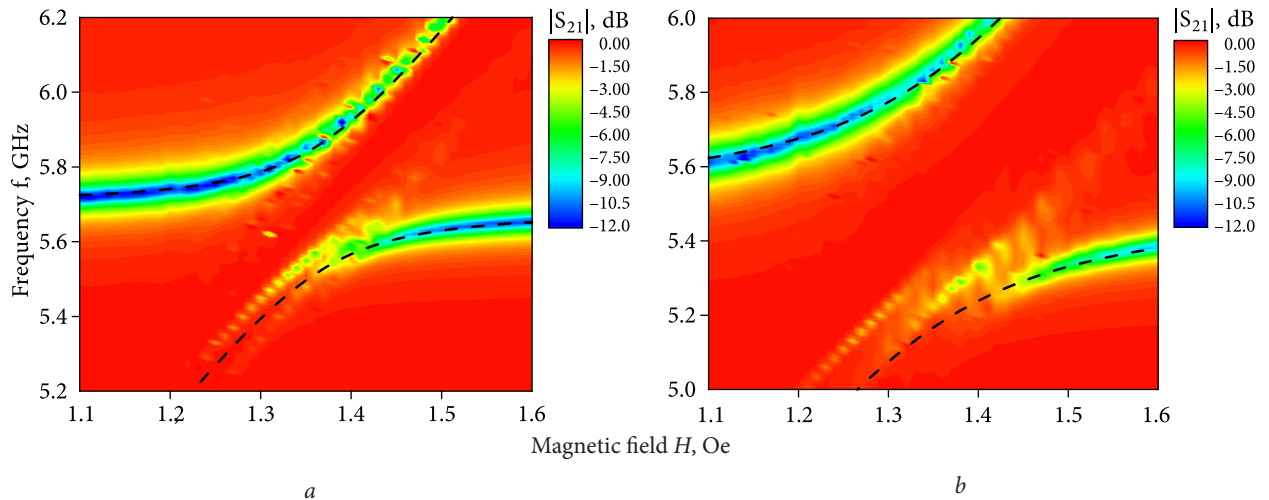
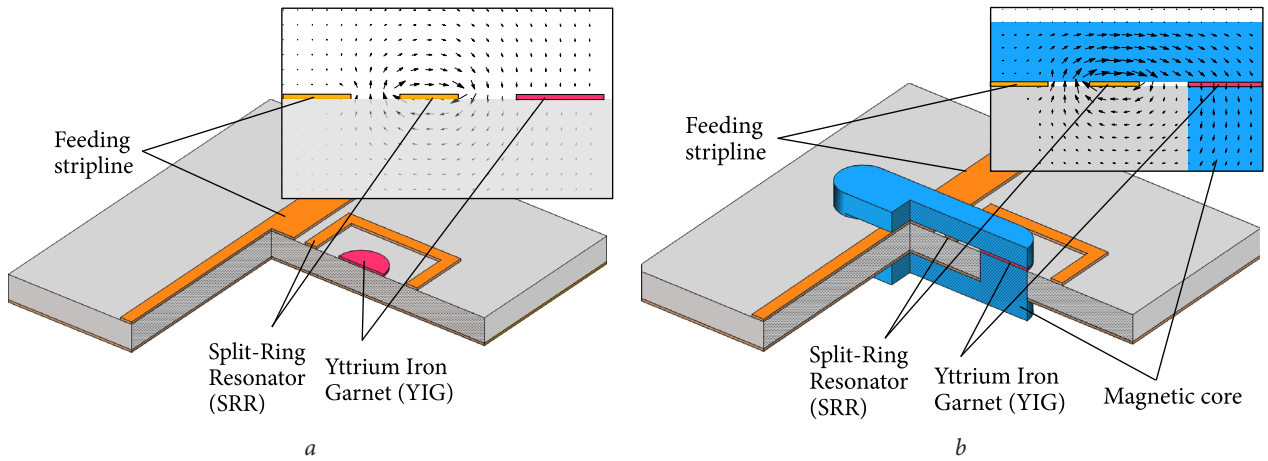
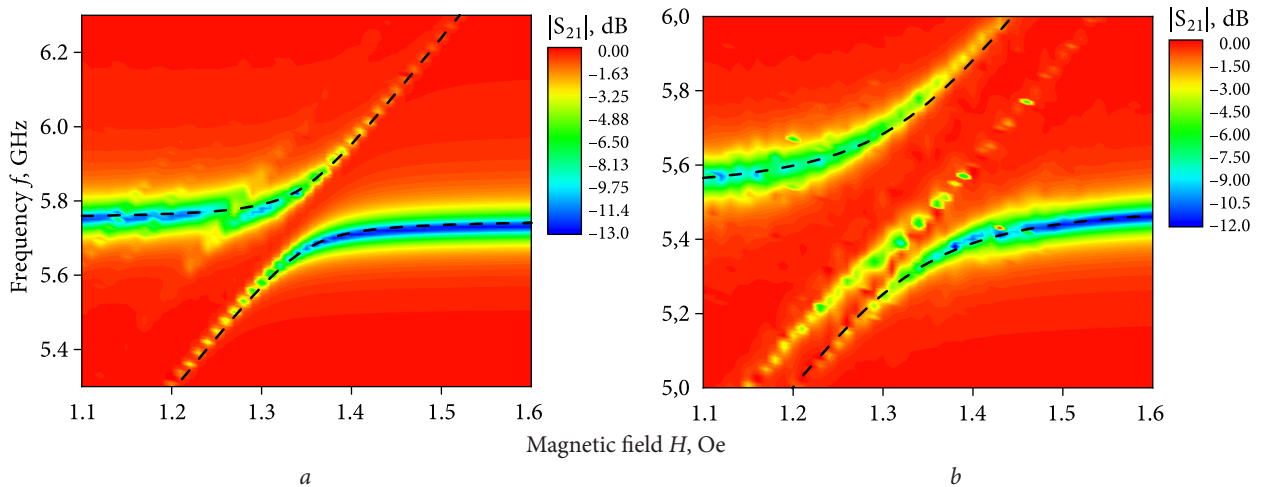


Fig. 4. Simulated transmission coefficient  $|S_{21}|$  spectra of waves propagating through the feeding stripline in the region of SRR-YIG coupled modes: *a* – without and *b* – with the magnetic core. The black dashed lines are dispersion curves calculated by formula (3)



**Fig. 5.** The SRR with feeding stripline and YIG film in the SRR center: *a* – without and *b* – with the magnetic core. The insets show the induction vector  $\vec{B}$  spatial distributions (black arrows) at the cross-section made by the  $yz$ -cutting plane in the YIG region and visualized with the parallelepiped-shaped cutout



**Fig. 6.** Simulated transmission coefficient  $|S_{21}|$  spectra of electromagnetic waves propagating through the feeding stripline in the region of the SRR-YIG coupled modes. The YIG film is in the SRR center: without the magnetic core (*a*) and in the narrow gap of the magnetic core (*b*)

In addition, we used the  $g/(2\pi)$  value and estimated the spin-number-normalized coupling strength by the formula  $g_N = g/(2\pi (N_s)^{1/2})$ , where  $N_s$  is the number of spins in the magnet volume. The concentration of spins for the YIG film was  $4.22 \cdot 10^{27} \text{ m}^{-3}$ . In the result,  $g/(2\pi) = 165 \text{ MHz}$  and  $g_N = 0.46 \text{ Hz}$  without the magnetic core (Fig. 4, *a*). With the magnetic core (Fig. 4, *b*),  $g/(2\pi) = 334 \text{ MHz}$  and  $g_N = 0.93 \text{ Hz}$ . Comparing the obtained  $g_N$  values with and without the magnetic core one finds that the P-M coupling strength for the SRR with the YIG film in the magnetic core presence is twice the P-M coupling strength without the magnetic core.

Fig. 5 illustrates the other scenario that the YIG film is inside the magnetic core in the SRR center. Again, a comparative study is conducted with and without the magnetic core, the same as for the scenario in Fig. 3. The magnetic core has a narrow gap ( $r = 0.035 \text{ mm}$ ), where the YIG film is placed. The gap of diameter  $d = 2.6 \text{ mm}$  is situated in the SRR center. Now, the YIG film is placed directly in the magnetic flux of the magnetic core. In this scenario, the YIG film is of cylindrical shape, its diameter is  $d = 2.6 \text{ mm}$ , and it fills the gap completely.

The YIG film presence in the gap reduces the average magnetic induction in the magnetic core. In this

scenario, the induction can be approximately estimated by the following expression [5]

$$B_c = \Phi/S = i\mu\mu_c/(l_c\mu + r\mu_c), \quad (4)$$

where  $i$  is the average current through the circuit,  $l_c$  is the average length of the magnetic core, and  $\mu = 1$  is the permeability of YIG material (beyond the FMR region) filling the gap,  $r = 0.035$  mm. We assume that the gap (where the YIG film is placed) and the magnetic core have the same cross-sectional area  $S$ . Yet, inside the gap itself, magnetic induction  $B$  and magnetic flux  $\Phi$  are larger than in the magnetic core absence. Notice, this increase is observed at a reasonably small  $r$ ,  $r^2 \ll S$  and at a sufficiently large relative permeability of the magnetic core,  $\mu_c \gg \mu$ . Thus, the P-M coupling strength efficiency in the region where the YIG film is placed increases considerably compared to the case without the magnetic core.

The numerical simulation results on the transmission spectra in the mode coupling region in the scenario that the YIG film is located in the SRR center with and without the magnetic core are presented in Fig. 6. As seen,  $g/(2\pi) = 87$  MHz when the YIG film is in the SRR center and the magnetic core is absent, and  $g/(2\pi) = 204$  MHz when the YIG film is in the narrow gap inside the magnetic core. Correspondingly, the calculated spin-number-normalized  $g_N$  value increases from 0.098 to 0.23 Hz. Thus, according to the simulation results, the  $g_N$  value increases more than 2.3 times in the magnetic core presence.

The analysis of  $g_N$  values in the scenarios in Figs. 3 and 5 puts forward an obvious statement that the condition  $\mu'' > 0$  met by the magnetic core material provides an estimated decrease of the  $g_N$  value, which is characteristic of the existing materials. It is not likely that the magnetic core will substantially increase the  $g_N$  parameter in planar resonators that feature high-concentration regions of alternating magnetic fields, e.g. in the inverse SRR [6]. However, as applied to planar resonators with a weak localization of the alternating magnetic field, the magnetic core can play an important role in the  $g_N$  increase.

## Conclusions

The transmission coefficient spectra of the split-ring resonator (SRR) in combination with a film of yttrium iron garnet (YIG) under the ferromagnetic resonance condition have been numerically simulated for the two scenarios of the YIG film location relative to the SRR: between the SRR and the feeding stripline (near the magnetic core) and in the SRR center (inside the magnetic core). In the first scenario, the spin-number-normalized coupling strength  $g_N$  increases up to 2.0 times when the magnetic core is present. In the second scenario, the  $g_N$  value increases more than 2.3 times. Importantly, the magnetic core introduction enlarges the spin-number-normalized coupling strength  $g_N$  at least 2.0 times.

**Acknowledgments.** This work was supported by the NATO Science for Peace and Security Programme, NATO SPS project No. G5859.

## REFERENCES

1. Biswanath, Bhoi, Sang-Koog, Kim, 2019. Photon-magnon coupling: Historical perspective, status, and future directions. *Solid State Phys.*, **70**, pp. 1–77. DOI: /10.1016/bs.ssp.2019.09.001
2. Pendry, J.B., Holden, A.J., Robbins, D.J., Stewart, W.J., 1999. Magnetism from conductors and enhanced nonlinear phenomena. *IEEE Trans. Microwave Theory Tech.*, **47**, pp. 2075–2084.
3. Dou, Y., Ouyang, Z., Thummala, P., and Andersen, M.A.E., 2018. PCB embedded inductor for high-frequency ZVS SEPIC converter. In: *2018 IEEE Applied Power Electronics Conference and Exposition (APEC)*, pp. 98–104. DOI: 10.1109/APEC.2018.8340994
4. Taylor, L., Margueron, X., Le Menach, Yv., Le Moigne, Ph., 2017. Numerical modelling of PCB planar inductors: impact of 3D modelling on high-frequency copper loss evaluation. *IET Power Electron.*, **10**(14), pp. 1966–1974. DOI: 10.1049/iet-pel.2017.0086
5. Fitzgerald, A.E., Kingsley JR., C., Umans, S.D., 2003. *Electric Machinery*. 6th ed. McGraw-Hill. ISBN-13: 978-0-07-053039-3, ISBN: 0-07-053039-4
6. Bhoi, B., Kim, B., Kim, J., Cho, Y.-J., Kim, S.-K., 2017. Robust magnon-photon coupling in a planar-geometry hybrid of inverted split-ring resonator and YIG film. *Sci. Rep.*, **7**, 11930. DOI: 10.1038/s41598-017-12215-8
7. Zhang, D., Song, W., Chai, G., 2017. Spin-wave magnon-polaritons in a split-ring resonator/single-crystalline YIG system. *J. Phys. D: Appl. Phys.*, **50**(20), 205003. DOI: 10.1088/1361-6463/aa68cf
8. Klingler, S., Maier-Flaig, H., Gross, R., Hu, C.-M., Huebl, H., Goennenwein, S.T.B., Weiler, M., 2016. Combined Brillouin light scattering and microwave absorption study of magnon-photon coupling in a split-ring resonator/YIG film system. *Appl. Phys. Lett.*, **109**(7), 072402. DOI: 10.1063/1.4961052
9. Tay, Z.J., Soh, W.T., Ong, C.K., 2018. Observation of electromagnetically induced transparency and absorption in Yttrium Iron Garnet loaded split ring resonator. *J. Magn. Mater.*, **451**, pp. 235–242. DOI: 10.1016/j.jmmm.2017.11.029

10. Bhoi, B., Cliff, T., Maksymov, I.S., Kostylev, M., Aiyar, R., Venkataramani, N., Prasad, S., Stamps, R.L., 2014. Study of photon-magnon coupling in a YIG-film split-ring resonant system. *J. Appl. Phys.*, **116**(24), 243906. DOI: 10.1063/1.4904857
11. Nicholson, D.B., 1990. Hexagonal ferrites for millimeter-wave applications. *Hewlett-Packard J.*, **41**(5), pp. 59–61.

Received 03.11.2023

A.C. Вакула<sup>1</sup>, С.Ю. Полевой<sup>1</sup>, К.Ю. Сова<sup>1,2</sup>,  
А.А. Гіріч<sup>1</sup>, С.І. Таранов<sup>1,2,3</sup>, С.В. Недух<sup>1</sup>

<sup>1</sup> Інститут радіофізики та електроніки ім. О.Я. Усикова НАН України  
вул. Акад. Проскури, 12, м. Харків, 61085, Україна

<sup>2</sup> Gebze Technical University  
2, Cumhuriyet Mah. 2254 St., 41400, Gebze/Kocaeli, Turkey

<sup>3</sup> Харківський національний університет імені В.Н. Каразіна  
майдан Свободи, 4, м. Харків, 61022, Україна

### ЗАСТОСУВАННЯ МАГНІТНОГО ОСЕРДЯ В ПЛАНАРНОМУ РЕЗОНАТОРІ З ПЛІВКОЮ ЗАЛІЗОГІРІЄВОГО ГРАНАТУ ДЛЯ ПІДСИЛЕННЯ ФОТОН-МАГНОННОГО ЗВ'ЯЗКУ

**Предмет і мета роботи.** У статті представлено результати чисельного моделювання спектрів пропускання резонатора з розділеним кільцем (РПК), навантаженого тонкою плівкою залізогрієвого гранату (ЗІГ). Запропоновано застосування магнітопроводу в РПК для підсилення фотон-магнітного (ФМ) зв'язку. Зареєстровано ефект антикросингу в поведінці частотної дисперсії мод РПК і феромагнітного резонансу плівки ЗІГ, а саме зв'язаних мод РПК-ЗІГ. Розмірні параметри РПК з магнітопроводом обчислюються з урахуванням компактності конструкції та прагнення отримати максимально можливу силу зв'язку, нормовану за числом спінів для такої системи. Робота спрямована на оцінку ефективності застосування магнітопроводу в складі планарного мікрохвильового резонатора для підсилення ФМ-зв'язку.

**Методи та методологія.** Чисельно досліджено спектри коефіцієнта пропускання  $|S_{21}|$  електромагнітних хвиль, що проходять через планарний резонатор із плівкою ЗІГ в умовах феромагнітного резонансу, за допомогою пакету CST Studio Suite в частотній області. Функція просторового розподілу напруженості магнітного поля розрахована для двох сценаріїв розміщення плівки ЗІГ: біля магнітопроводу (між РПК та смужковою лінійкою) і всередині магнітопроводу (в центрі РПК). Крім того, для кожного з цих двох сценаріїв було промодельовано спектри коефіцієнта пропускання  $|S_{21}|$  хвиль, що розповсюджуються через смужкову лінію в області зв'язаних мод РПК-ЗІГ за наявності магнітного осердя і без нього. Дисперсійні криві зв'язаних мод РПК-ЗІГ було отримано в аналітичній формі.

**Результати.** Показано, що при застосуванні магнітопроводу сила ФМ-зв'язку збільшується вдвічі за умови розташування плівки ЗІГ поблизу магнітопроводу (між РПК і смужковою лінійкою). Коли плівка ЗІГ знаходиться всередині магнітного осердя (у центрі РПК), сила ФМ-зв'язку збільшується в 2.3 рази порівняно з аналогічними випадками без магнітного осердя.

**Висновки.** Застосування магнітного осердя в резонансній системі «РПК — магнітна плівка» дає можливість збільшувати силу ФМ-зв'язку для розробки ефективних перетворювачів хвиль НВЧ-діапазону в оптичний та забезпечення якісного обміну інформацією між квантовими комп'ютерами.

**Ключові слова:** фотон-магнітний зв'язок, планарний резонатор, феромагнітний резонанс, спектри пропускання, магнітопровід.